Characterization of Air Entrainment and Mixture Formation Processes of Multi-Hole Injector Spray for Diesel Engine: Comparison with Single-Hole Injector

Shinichi Kakami*[1], Jaeheun Kim[1], Yu Jin[1], Keiya Nishida[1], Yoichi Ogata[1]
Graduate School of Engineering, [1]University of Hiroshima, Higashi-Hiroshima, Japan
*Corresponding author: m180359@hiroshima-u.ac.jp

Abstract

A comparison of spray characteristics between single-hole and multi-hole injectors were conducted under same rail pressure condition of 100MPa or similar injection rate profile condition. The same injection rate profile was achieved by adjusting the rail pressure. Laser absorption scattering (LAS) technique was implemented for measuring the mixture concentration distribution. Injection quantities of 2.5mg and 0.5mg were selected to realise quasi-steady state and transient spray, respectively. In case of quasi-steady spray and same rail pressure condition, the difference in terms of mixture distribution between single-hole and multi-hole injector was not significant under 2.5mg condition. This is because the quasi-steady spray played dominant role over the injection process. However, in case of transient spray condition, single-hole injector showed the longer vapor penetration but smaller spray angle than that of multi-hole injector. Nevertheless, the single-hole injector showed the faster lean mixture formation after start of injection than that of multi-hole injector. However, at the end-of-injection (EOI) timing, the single-hole injector showed slower evaporation rate. The air entrainment characteristics of both injectors were assessed using a 1D spray model. The propagation speed of the relative entrainment rate was greater for single-hole than that of multi-hole injector. It contributed in leaner mixture formation for single-hole injector after EOI. Under the similar injection rate profile condition, the vapor penetration was almost identical for both injectors. However, multi-hole injector showed the wider spray angle than that of single-hole injector. Therefore, the multi-hole injector showed the leaner mixture distribution and faster evaporation rate than that of single-hole injector. In summary, for the transient spray condition, the single-hole injector was advantageous on the air entrainment under the same rail pressure, whereas the multi-hole injector was advantageous under similar injection rate profile.

Keywords

Diesel spray, Laser absorption scattering (LAS), Mixture formation, Air entrainment

Introduction

Diesel engines have the advantage of their high thermal efficiency and low CO_2 emission compared to gasoline engines. However, NO_x and soot emissions are serious problem. The fuel/air mixture formation process inside the combustion chamber affects directly on the engine performance and emission formation process. Therefore, it is important to investigate the mixture formation process of the diesel spray.

Recently, several visualization experiments are conducted under engine-like conditions using optical method such as Laser absorption scattering technique (LAS), Laser induced fluorescence (LIF), Laser induced exciplex fluorescence (LIEF), and Rayleigh scattering technique. Because of the difficulty of optical access and simplification of the physical phenomenon, single-hole injector is widely used instead of multi-hole injector. However, multi-hole injector is used in real engine in order to spread the fuel efficiently inside the combustion chamber.

Some researches were conducted to clarify the difference between single-hole and multi-hole injector under large injection quantity condition where the injection rate profiles have reached the quasi-steady state [1]. However, small injection quantity condition where the entire injection profiles are under transient, are rarely conducted.

The small injection quantity conditions are widely used in the multiple injection strategies since it is effective way to reduce the combustion noise and emission formation [2]. Therefore, it is important to understand the difference between single-hole and multi-hole injector under small injection quantity as well as large injection quantity.

The main objective of this research is to investigate the mixture formation of large and small injection quantity with single-hole and multi-hole injector. In this regard, the experiments are conducted under both same rail pressure condition and similar injection rate profile condition. LAS technique is utilized to observe the mixture formation process. 1D spray model is utilized to clarify the mixture formation and air entrainment characteristics difference.

Principle of LAS (Laser Absorption Scattering) technique

The principle of LAS, which is used in the current study for acquiring mixture distribution, will be explained briefly. The LAS technique utilizes ultraviolet (UV) and visible wavelength laser, and the fuel concentration is determined

by the attenuation of these lights. The intensity of the visible light is only attenuated by the droplets scattering, while that of ultraviolet (UV) light is attenuated by both the droplets scattering, as well as the liquid and vapor absorption. However, the liquid absorption of the UV light can be negligible due to its weak signal [3]. Therefore, $log(I_0/I_t)_A$ and $log(I_0/I_t)_T$ which represent the UV and visible light attenuation respectively can be defined as in Eq. (1) and (2).

$$log\left(\frac{I_0}{I_t}\right)_{\lambda_A} = log\left(\frac{I_0}{I_t}\right)_{L_{sca}} + log\left(\frac{I_0}{I_t}\right)_{V_{abs}} \quad (1)$$

$$log\left(\frac{I_0}{I_t}\right)_{\lambda_T} = log\left(\frac{I_0}{I_t}\right)_{L_{sca}} \quad (2)$$

where the $log(I_0/I_t)_{Lsca}$ and $log(I_0/I_t)_{Vabs}$ represent the attenuation by the liquid scattering and vapor absorption respectively. The vapor absorbance is obtained through the Lambert-Beer's Law as in Eq. (3).

$$\log\left(\frac{I_0}{I_t}\right)_{V_{abs}} = \frac{\varepsilon C_v l}{M} \times 10^2 \quad (3)$$

where l *[m]* is the (line-of-sight) optical path length, ε [L/mol · cm] is the molar absorption coefficient, and C_v [kg/m^3] is the mass concentration of vapor per unit volume. Molar absorption coefficient is measured in a separate chamber for the calibration. The line-of-sight optical path is obtained through 'onion-peeling method' which will be explained later.

Finally, mass concentration of the vapor phase is obtained by combining Eq. (1) and (2) as shown in Eq. (4).

$$C_v = M\left[log\left(\frac{I_0}{I_t}\right)_{\lambda_A} - log\left(\frac{I_0}{I_t}\right)_{\lambda_T}\right] \times \frac{1}{\varepsilon l \times 10^2} \quad (4)$$

The onion-peeling method was applied to obtain the optical path length l in Eq. (3). First of all, the spray plume was assumed to be axisymmetric in order to apply the onion-peeling method. The basic idea of onion-peeling method is to obtain the fuel concentration from the most outer ring. Afterwards, the optical thickness of the second most outer ling is analysed through the fuel concentration results obtained from the most outer ring. Mixture temperature is also calculated through the conservation of enthalpy as written in Eq. (5).

$$C_{p,air} m_{air}\left(T_{amb} - T_{mix}\right) = m_{fuel}\left[C_{p,liquid}\left(T_b - T_f\right) + h_{fg} + C_{p,vapor}(T_{mix} - T_b)\right] \quad (5)$$

The mixture temperature and the vapor mass (as well as vapor concentration) are obtained through iteration based on Eq. (4) and (5). This process is repeated until the most inner ring and eventually every layers of the ring are de-convoluted. The vapor mass inside spray volume can be obtained based on axisymmetric spray assumption by multiplying the vapor mass of each pixel by π· radius. The entrainment air mass is also calculated using the information of the fuel mass, volume and mixture temperature in each unit volume since density of the fuel and ambient gas were obtained if the mixture temperature is known. This process is repeated until the most inner ring and eventually every layer of the ring will be de-convoluted. A more precious and detailed description can be found in [4].

In order to assume an axisymmetric spray and utilize onion-peeling method, the spray plume should be perpendicular to the laser beam. It is easy to realize these optical requirements for single-hole injector. However, the dedicated adaptor is required for multi-hole injector to satisfy these requirements. The injector was tilted with a certain angle so that one of the seven spray to be the perpendicular to the laser as depicted in Figure 1. There are some visibility limitations at the vicinity of the nozzle due to the configuration of this injector adaptor. The spray tip area of around 9 mm downstream of the nozzle hole was excluded during the image processing since the boundaries of the adaptor and the vicinity of the nozzle become blur at high temperature, high pressure condition and may yield uncertainty. Therefore, only clear area depicted in green window in the Figure 1 was used for the analysis.

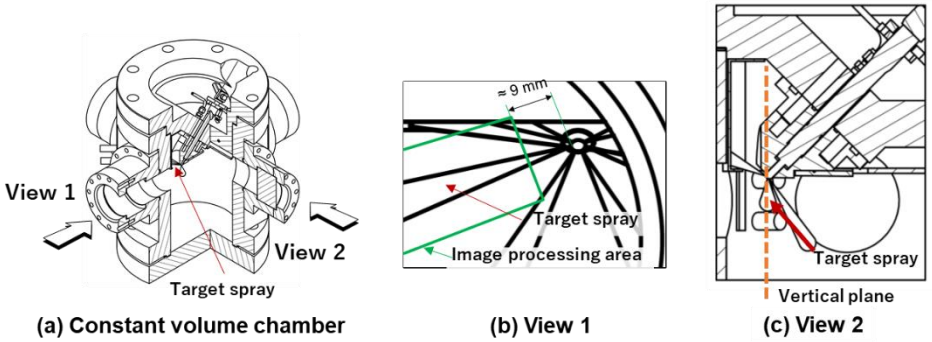

Figure 1. Installation of multi-hole injector in constant volume chamber for axisymmetric spray observation.

Experimental setup and conditions

Figure 2 shows the schematic diagram of the experimental apparatus. A pulsed Nd-YAG laser (LOTIS TII LS-2137N), and two CCD-cameras (ANDOR iKon-M Series) are used for the optical system. The wavelength for UV and visible light are 266 nm and 532 nm, respectively. These laser beams are first expanded to a size of a similar diameter to the quartz window of the chamber. The laser beams are merged and passes through the chamber and the spray. Finally, the attenuated beams are separated by a harmonic separator and received by CCD cameras corresponding to their wavelengths. For each injection event, a background and a spray image are taken with an interval of the 0.5 seconds, in order to prevent any noise during the image processing. The interval between the injection and the imaging timing (triggers for laser and cameras) are controlled by the delay generator (LabSmith LC880 programmable Experiment Controller).

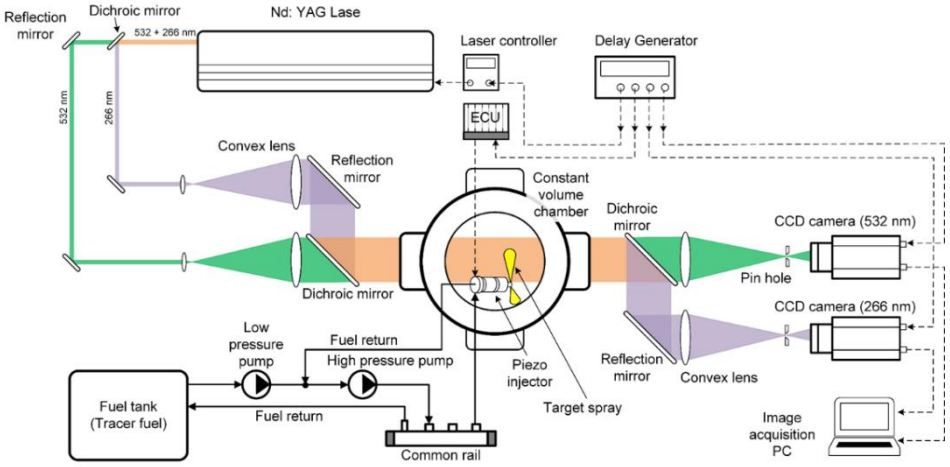

Figure 2. Laser absorption scattering (LAS) optical system, injection system and constant volume chamber.

The specifications of the injectors used in this study and experimental conditions are listed in Table 1. The geometry of the nozzle is identical for both injectors. Both same rail pressure condition and similar injection rate profile condition were conducted. In case of same rail pressure condition, injection quantities of 2.5mg and 0.5mg were selected to realize quasi-steady state and transient spray, respectively. Similar injection rate profile condition was achieved by adjusting the rail pressure of single-hole injector. Only small injection quantity condition was selected for similar injection rate profile condition since it was not possible to achieve the similar injection rate profile for large injection quantity. Injection rate profile was measured using Zeuch method [5] prior to the LAS experiment. The measured injection rate profiles of both same rail pressure and similar injection rate profile conditions were also shown in figure 3.

Table 1. Specifications of the injectors and summarized experimental conditions.

Injector specifications		
	Single-hole	Multi-hole
Injector type	Piezo actuator type	
Number of holes	1	7
Nozzle hole diameter [mm]	0.123	0.123
Umbrella angle [deg]	-	155
Ambient condition		
Ambient density [kg/m^3]	8.42	
Ambient pressure [MPa]	2.00	
Ambient temperature [K]	800	
Ambient gas component	Nitrogen	

Under same rail pressure condition		
	Single-hole	Multi-hole
Injection pressure [MPa]	100	
Injection quantity [mg]	0.5, 2.5	
Under similar injection rate pfofile condition		
Injection pressure [MPa]	30	100
Injection quantity [mg]	0.53	0.59

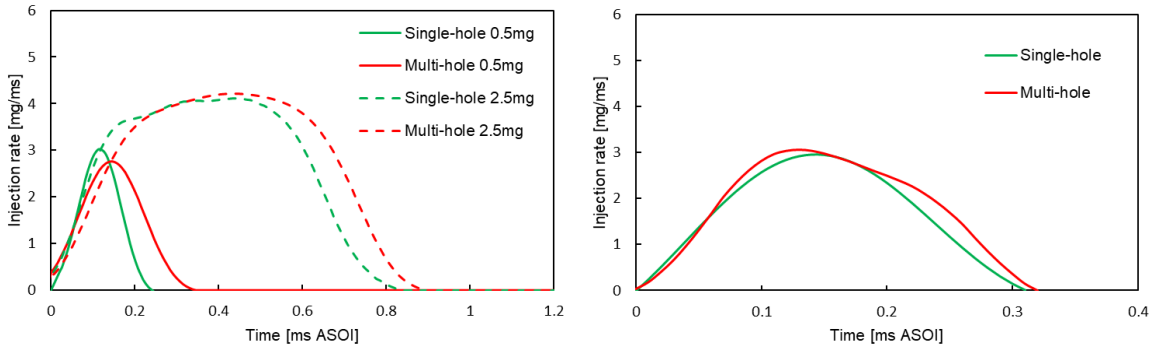

(a) Same rail pressure condition (b) Similar injection rate profile condition

Figure 3. Injection rate profiles under same rail pressure condition (a) and similar injection rate profile condition (b).

Results and discussion

Same rail pressure condition

Figure 4 shows the vapor penetration and spray angle with injection rate profile for both injectors. The increase rate of the injection rate was faster for single-hole injector due to the faster pressure build-up inside the sac room [1]. Due to the faster increase of injection rate, single-hole injector showed the greater vapor penetration for both injection quantities right after start of injection. In case of injection quantity of 2.5mg, the difference of vapor penetration between both injectors become smaller as time elapse. For large injection quantity condition, which reaches the quasi-steady state, there was no obvious difference of the peak value of injection rate for both injectors. Similar peak value of injection rate means similar momentum of the spray, which results in similar vapor penetration except for right after start of injection. However, in case of injection quantity of 0.5mg, whole injection process did not reach the quasi-steady state as shown in the injection rate profile and single-hole injector showed greater vapor penetration during whole injection process. The spray angle shows the same tendency with penetration results, which is the obvious difference occurred only in case of injection quantity of 0.5mg. For multi-hole injector, the drastic velocity changes and swirling motion happens inside the sac room and nozzle, which can generate cavitation. This complex flow structure increased the turbulence intensity and vortices, and it created the higher degree of radial velocity in the multi-hole injector [1]. These phenomena became obvious under the injection quantity of 0.5 mg. Therefore, the difference between single- and multi-hole injectors was more pronounced.

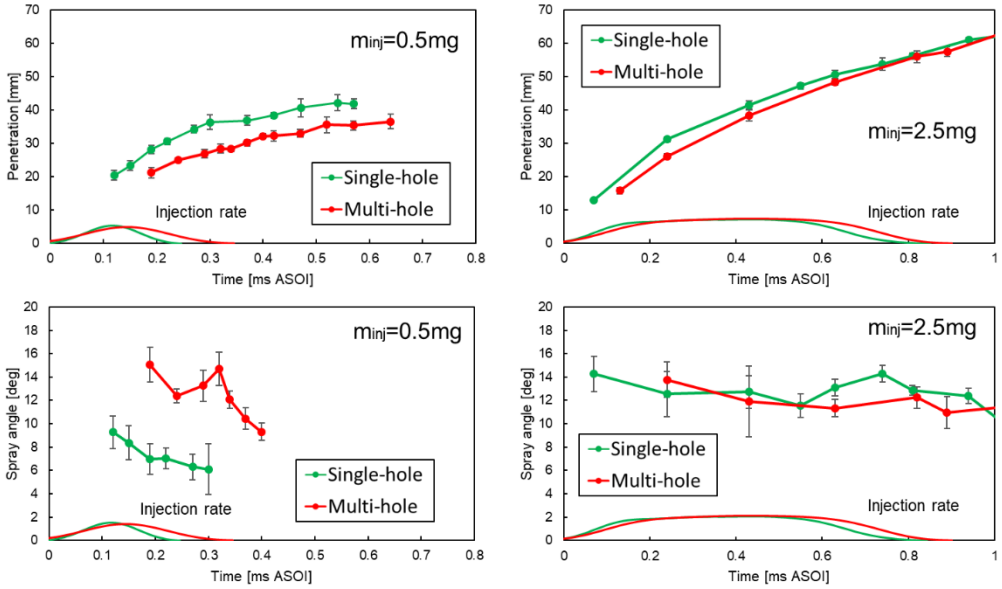

(a)m_{inj}=0.5m (b)m_{inj}=2.5mg

Figure 4. Vapor penetration (upper) and spray angle (below) between single- and multi-hole injectors.

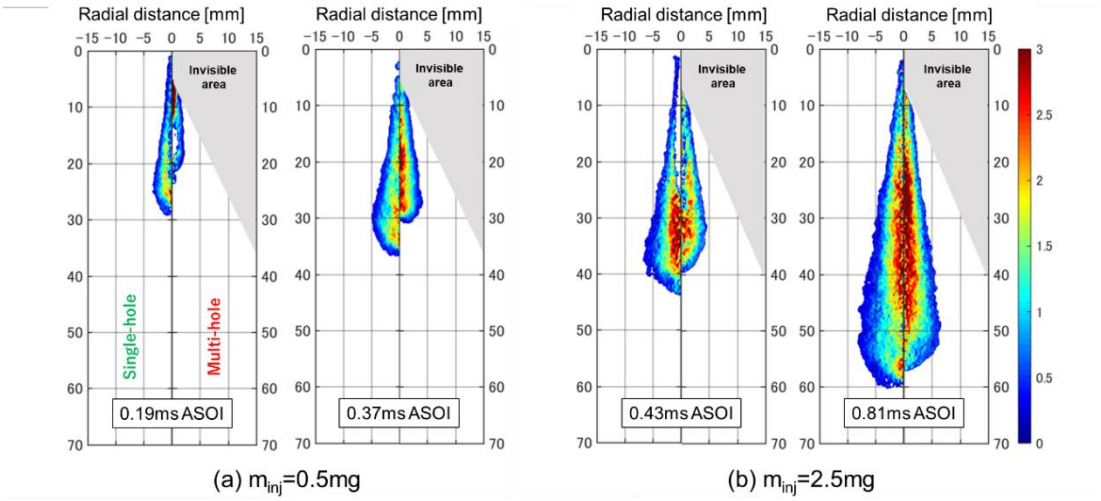

(a) m_{inj}=0.5mg (b) m_{inj}=2.5mg

Figure 5. Vapor equivalence ratio distribution.

The vapor equivalence ratio distribution for both injection quantities were shown in Figure 5. In each figure, left portion of the image represents the results of single-hole injector, while right portion of the image shows the results of multi-hole injector. For large injection quantity condition shown in Figure 5(b), the equivalence ratio distribution of both injectors was similar. The quasi-steady state spray played dominant role over the injection process and there was no significant difference on spray structure and mixture formation for both injectors. On the other hand, for small injection quantity condition, single-hole injector showed the leaner mixture formation. The ratio of entrainment air and injected mass was shown in Figure 6. The injected mass at each timing was obtained from the integration of the injection rate. Generally, wider spray angle means enhancing the lean mixture formation. However, in this case, longer vapor penetration for single-hole injector was able to overcome the disadvantage of its smaller spray angle and enhance the air entrainment.

Evaporation ratio versus time under injection quantity of 0.5mg were shown in Figure 7. In order to eliminate the EOI timing effect on mixture formation, these results were aligned to EOI timings of each injector. Although the lean mixture was formed for single-hole injector when aligned to SOI timing as discussed above, the evaporation ratio (vapor mass / total mass) showed slower development as depict in Figure 7. At the EOI timing, the evaporation ratio of single-hole injector is around 40%, on the other hand, that of multi-hole injector was around 80%. When compared the liquid phase image at the right after the end of injection timing (0.01msAEOI) shown in Figure 8, single-hole injector showed dense liquid core compared to multi-hole injector. Figure 9 shows the total fuel concentrations in the direction of spray axis at different timings after end of injection. The total fuel concentration was calculated by the following equation,

$$\bar{C}(x)_{total} = \frac{m(x)_{liquid} + m(x)_{vapor}}{V(x)_{vapor}} \tag{6}$$

where the $\bar{C}(x)_{total}$ is the mean total fuel concentration at each axial location; $m(x)_{liquid}$ and $m(x)_{vapor}$ are the liquid and vapor total mass at each axial location respectively; $V(x)_{vapor}$ is the vapor volume at each axial location. For multi-hole injector, it is not possible to observe within the 9 mm downstream from the nozzle tip as discussed above. Thus, the area below 10mm from the nozzle tip was excluded in the figure 9. At the 0.01ms AEOI, single-hole showed the much higher concentration near the nozzle tip area. This can be explained from the liquid core region formed with single-hole injector shown in Figure 9. However, the concentration difference became smaller rapidly at the 0.04ms AEOI. Finally, the concentration of single-hole injector caught up with that of multi-hole injector near the nozzle tip region shown at the 0.09ms AEOI.

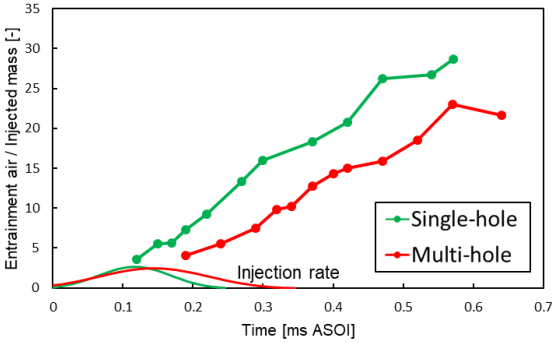

Figure 6. Ratio of entrainment air and injected mass under injection quantity of 0.5mg.

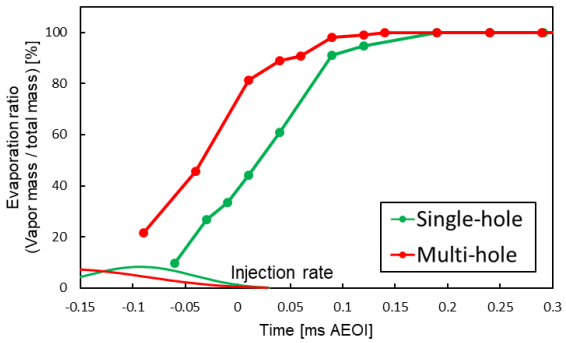

Figure 7. Evaporation ratio versus time under injection quantity of 0.5mg.

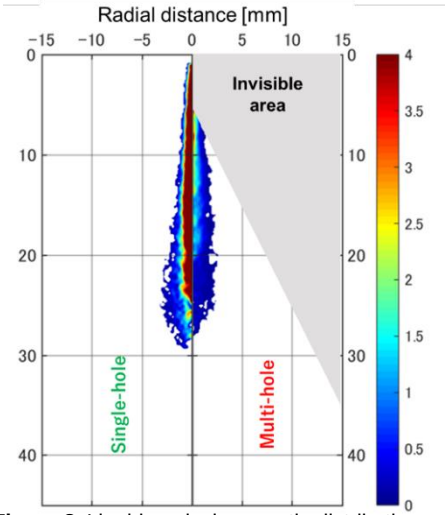

Figure 8. Liquid equivalence ratio distribution. (0.01ms AEOI)

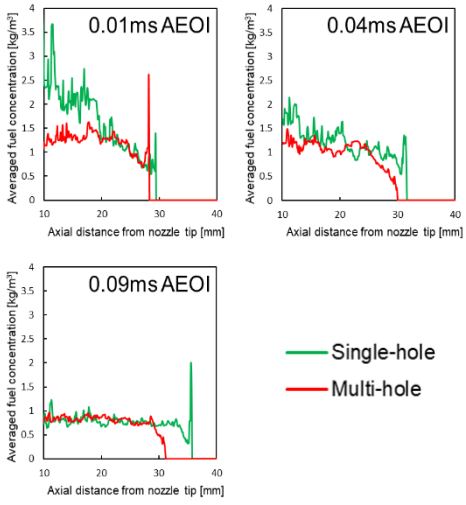

Figure 9. Mean fuel concentration distribution along the spray axis after EOI.

The vapor fuel distribution histogram was generated in a cumulative fashion from the equivalence ratio distribution images with a bin equivalence size of 0.05 and is shown in Figure 10. Single-hole injector showed the leaner mixture distribution at 0.01ms AEOI and this is due to the lower evaporation ratio as discussed above. However, single-hole injector still showed the leaner mixture formation even in the almost fully evaporating timing (0.09ms AEOI). For these results, single-hole injector seems to show the greater air entrainment compared to multi-hole injector after the end of injection.

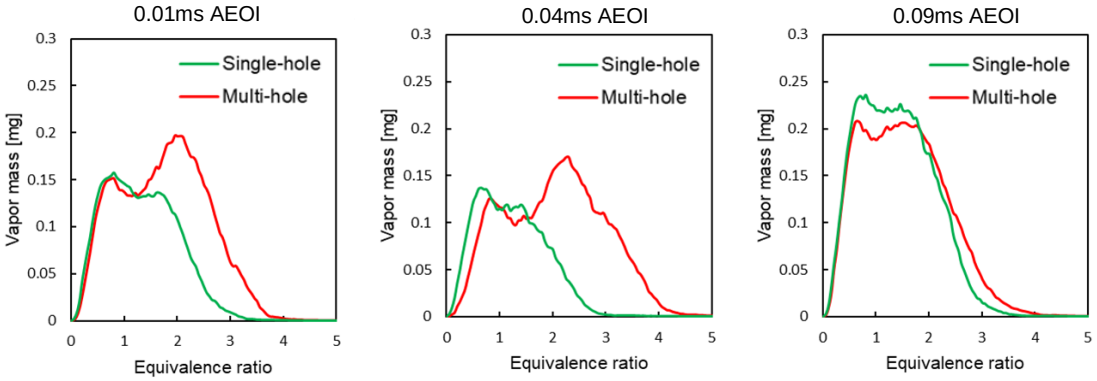

Figure 10. Vapor mass distributions versus equivalence ratio after EOI under injection quantity of 0.5mg.

In order to consider to these reasons, the air entrainment characteristics of both injectors were derived using the 1D model proposed in [6]. The emphasis is on the jet behaviour after the end of injection on this model. The detailed theory of this model was explained also in [6]. This model requires injection rate profile and spray angle. The spray angle at the end of injection was used as input spray angle for both injectors same as discussed in [7]. The relative entrainment rate is defined as the local instantaneous air entrainment rate divided by the air entrainment rate of a steady jet. Thus, a value of unity indicates the local entrainment rate is the same as for a steady jet. The relative air entrainment rate per unit fuel for both injectors were shown in Figure 11. The propagation speed of the peak value of relative entrainment per unit fuel and the peak value itself was around 1.5 times faster and greater for single-hole injector and it is explained from the injection rate profile. The injection rate for single-hole injector showed the faster decreasing before the EOI. When the decrease of fuel mass flux occurred, the entrainment mass flux needs to be increase in order to fulfil the momentum conservation. Faster decrease of the injection rate leads to increase the entrainment mass flux. Single-hole injector showed the leaner mixture distribution despite the liquid core region existing right after end of injection because of this strong entrainment flux.

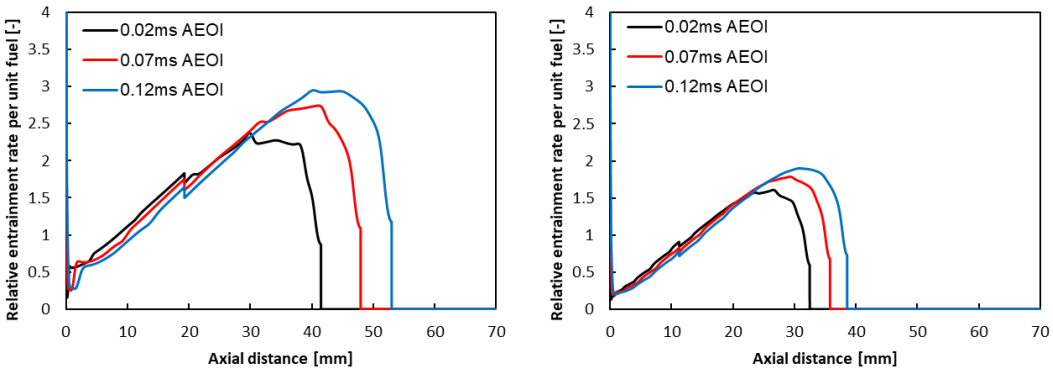

(a) Single-hole injector (b) Multi-hole injector

Figure 11. Relative air entrainment rate per unit fuel between single-hole and multi-hole injector.

Similar injection rate profile condition

For small injection quantity condition, the pressure inside the sac room of single-hole and multi-hole injectors are different as shown in the difference of injection rate profile in Figure 3. To exclude the effect of the injection rate profile difference and focus on the mixture formation comparison between single-hole and multi-hole injectors, similar injection rate profile was needed to be achieved. When the rail pressure of single-hole injector was 30MPa, similar injection rate profile (increasing rate, decreasing rate and peak value etc.) was achieved. Similar injection rate profile means similar injected fuel mass flux. Same sac pressure can be assumed if the discharge coefficient of two injectors are same.

The vapor penetration and spray angle was shown in Figure 12 with the injection rate profile. The vapor penetration was almost identical for both injectors. However, the greater spray angle was observed for multi-hole injector. The equivalence ratio distribution and vapor mass distribution were shown in Figure 13, 14, respectively. At the end of injection timing (0.32ms ASOI), multi-hole injector shows rich mixture due to the faster evaporation than that of single-hole injector since the greater spray angle of multi-hole injector enhances the air entrainment. Consequently, as the time elapse, single-hole injector showed the leaner mixture formation as shown in Figure 13 (0.52ms ASOI). The similar injection rate profile means similar decreasing rate of fuel mass flux just before the EOI. Therefore, the single-hole injector was not possible to make the leaner mixture formation than multi-hole injector even after EOI timing unlike the case of same rail pressure condition.

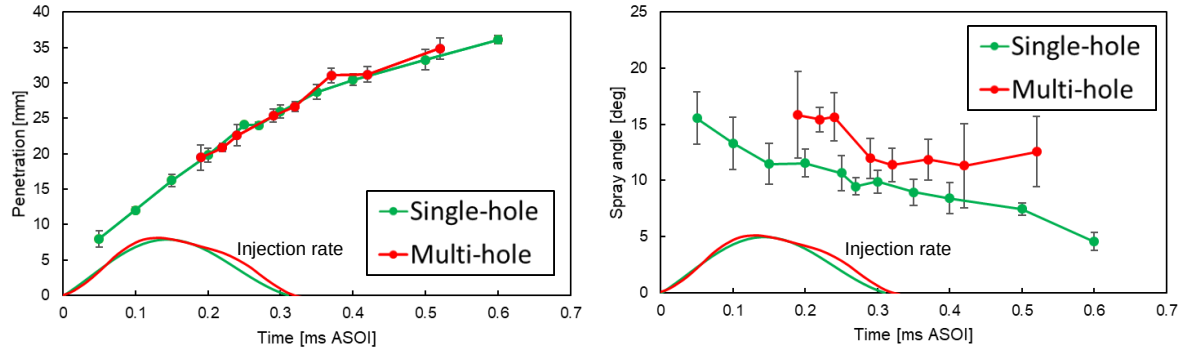

(a) Vapor penetration (b) Spray angle

Figure 12. Vapor penetration (a) and spray angle (b) with injection rate profile.

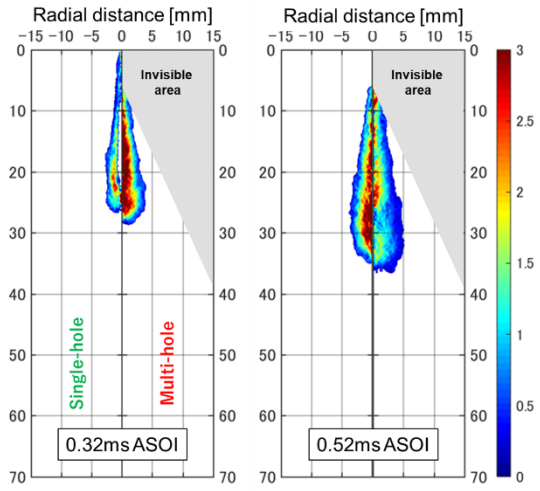

Figure 13. Vapor equivalence ratio distributions under similar injection rate profile.

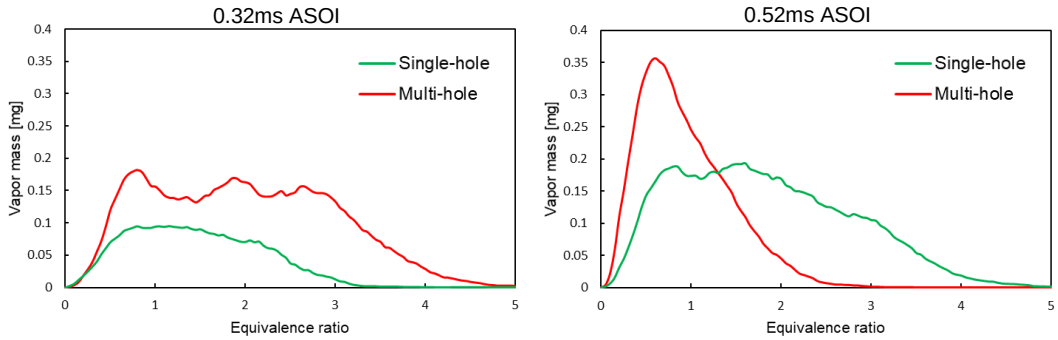

Figure 14. Vapor mass distributions versus equivalence ratio after EOI under injection quantity of 0.5mg.

Conclusions

The investigation on the spray characteristics of small (0.5mg/hole) and large (2.5mg/hole) injection quantities with single-hole and multi-hole injectors were conducted. The mixture formation and air entrainment characteristics were compared between two injectors.

1. When aligned the start of injection timing, single-hole injector showed the leaner mixture due to the longer penetration than that of the multi-hole injector. The longer penetration of single-hole injector was able to overcome the disadvantage of its smaller spray angle. However, the difference between two injectors was obvious only under small injection quantity condition. For large injection quantity condition, quasi-steady state spray played dominant role over the whole injection process and the difference became smaller.
2. The evaporation ratio of multi-hole injector was higher than that of single-hole injector at the end of injection timing. Single-hole injector showed the dense liquid core at the EOI timing. However, the fuel concentration distribution results along the spray axis showed rapid decrease of mean fuel concentration near the nozzle for single-hole injector. 1D simulation results showed that the relative entrainment rate per unit fuel was around 1.5 times faster with single-hole injector due to the rapid decrease of the injection rate profile. This led the faster lean mixture formation for single-hole injector after EOI timing.
3. Similar injection rate profile of both injectors was achieved by adjusting the injection pressure of the single-hole injector. In this way, the vapor penetration was almost identical for both injectors. The multi-hole injector showed the greater spray angle than that of single-hole injector. This greater spray angle enhanced the air entrainment and led the faster lean mixture formation for multi-hole injector.

Acknowledgements

This work was supported by the Council for Science, Technology and Innovation (CSTI), Cross-ministerial Strategic Innovation Promotion Program (SIP), “Innovative combustion technology” (funding agency: JST)

Nomenclature

SOI : Start of injection
EOI : End of injection
CCD : Charge-coupled device
I_0 : Incident light
I_t : Transmitted light
M : Molar mass
$C_{p,air}$: Constant pressure specific heat of air
$C_{p,liquid}$: Constant pressure specific heat of liquid fuel
$C_{p,vapor}$: Constant pressure specific heat of vapor fuel
h_{fg} : Latent heat of evaporation
T_{amb} : Ambient temperature
T_{mix} : Mixture temperature
T_b : Boiling temperature of fuel
T_f : Initial fuel temperature of fuel

References

[1] Dong, P., Inaba, T., Nishida, K., Ogata, Y. et al., "Characteristics of Nozzle Internal Flow and Near-Field Spray of Multi-Hole Injectors for Diesel Engines," SAE Technical Paper 2015-01-1920, 2015.
[2] Busch, S., Zha, K., Miles, P.C., 2015, International Journal of Engine Research, 16 (1), pp. 13-22.
[3] Matsuo, T., Li, K., Itamochi, M., Nishida, K. et al., Oct. 26.-29. 2014, 17th Annual conference on liquid atomization and spray systems – Asia.
[4] ZHANG, Y., NISHIDA, K., and YOSHIZAKI, T., "Quantitative Measurement of Droplets and Vapor Concentration Distributions in Diesel Sprays by Processing UV and Visible Images," SAE Technical Paper 2001-01-1294, 2001.
[5] Bower, G. and Foster, D., "A Comparison of the Bosch and Zuech Rate of Injection Meters," SAE Technical Paper 910724, 1991.
[6] Musculus, M. and Kattke, K., "Entrainment Waves in Diesel Jets," SAE Int. J. Engines 2(1):1170-1193, 2009.
[7] Kook, S., Pickett, L., and Musculus, M., "Influence of Diesel Injection Parameters on End-of-Injection Liquid Length Recession," SAE Int. J. Engines 2(1):1194-1210, 2009.